Supplemental Table of Content

Table S1. List of normal and HGPS skin fibroblasts from National Institute of Aging (NIA) repository

Skin fibroblasts from NIA repository	Phenotype	Age	Sex	Race	Passage No. in the Exp	Number of cells quantified in Fig. 6 (siControl/siSUN1)
AG03512	Normal	41	F	Caucasian	4-6	(199/193)
AG03257	Normal	35	F	Caucasian	N/A+(1-3)	(140/172)
AG03258	Normal	36	M	Caucasian	N/A+(1-3)	(116/177)
AG08469	Normal	38	M	Caucasian	4-6	(138/171)
AG01972	HGPS (1824C>T, G608G)	14	F	Caucasian	13-15	(154/183)
AG06297	HGPS (1824C>T, G608G)	8	M	Caucasian	20-22	(133/189)
AG11498	HGPS (1824C>T, G608G)	14	M	African	7-9	(163/196)
AG11513	HGPS (1824C>T, G608G)	8	F	Caucasian	7-9	(123/153)
AG06917	HGPS (1824C>T, G608G)	3	M	Caucasian	15	N/A
AG03513	HGPS (1824C>T, G608G)	13	M	Caucasian	10	N/A
AG03198	HGPS (1824C>T, G608G)	10	F	Caucasian	9	N/A

cPDL: cumulative population doubling level; N/A: not attempted

SUPPLEMENTAL FIGURES & LEGENDS

Suppl Figure S1.

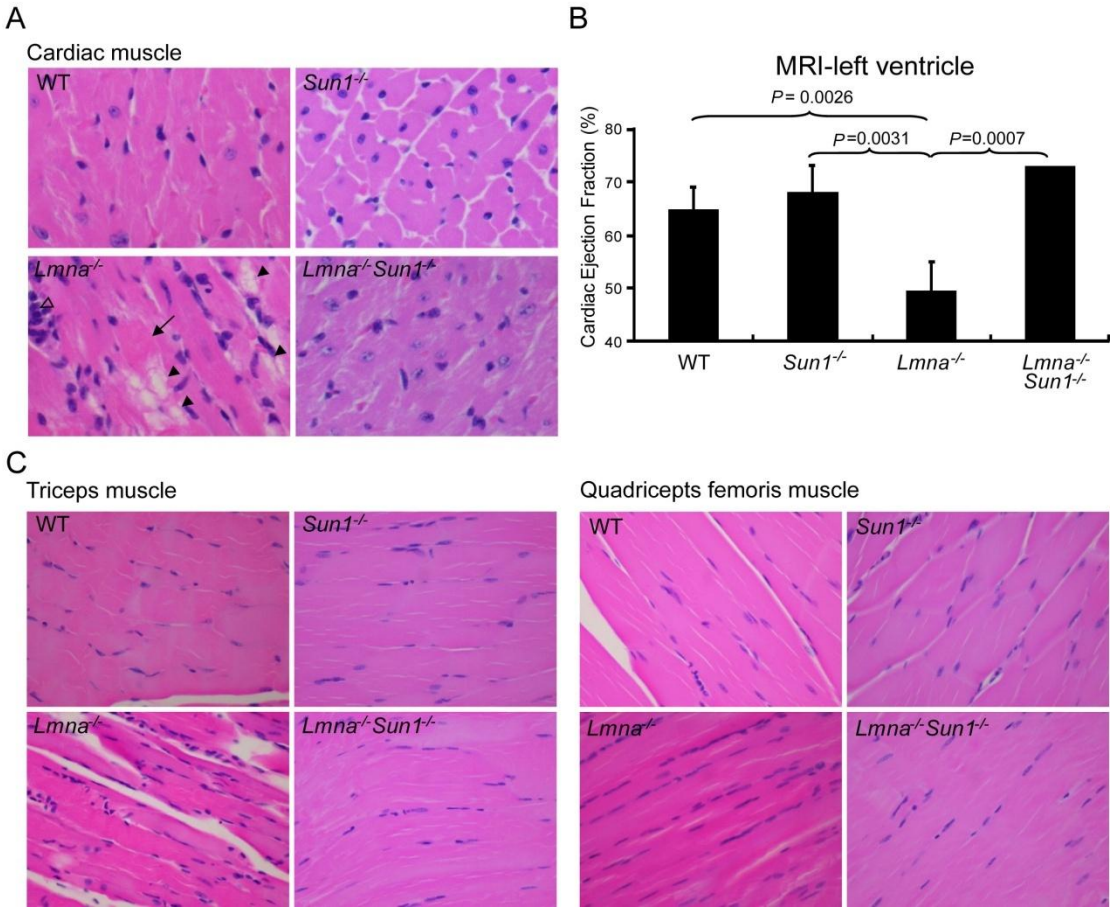

Supplemental Figure S1. **Multiple tissue defects in *Lmna*$^{-/-}$ mice are ameliorated in *Lmna*$^{-/-}$*Sun1*$^{-/-}$ double knockout mice (related to Figure 2).**

(A) Hematoxylin and eosin (H&E) -stained sections of tissues from 5-6 week old mice. In each case, *Lmna*$^{-/-}$*Sun1*$^{-/-}$ tissues are improved in pathology over *Lmna*$^{-/-}$ counterparts. Cardiac muscle: *Lmna*$^{-/-}$ cardiac muscle showed more tissue vacuoles than WT, *Sun1*$^{-/-}$, or *Lmna*$^{-/-}$*Sun1*$^{-/-}$ muscle (600× magnifications). Hollow triangle: infiltrates of lymphocytes and neutrophils, solid triangle: sarcoplasmic vacuoles, arrow: myocyte necrosis.

(B) Cardiac function: Abnormal cardiovascular functions were found in the *Lmna*$^{-/-}$ mice; the left ventricle ejection fraction as indicated in the "Cardiovascular Parameters" was measured by MRI (magnetic resonance imaging). Values are mean+/-SD.

(C) Tricep muscle and quadricep femoris muscle: the musculature of *Lmna*$^{-/-}$ mice contains smaller myocytes; the nuclei are closer together, and the myocytes adjacent to the bone are significantly atrophied (600× magnifications).

Suppl Figure S2.

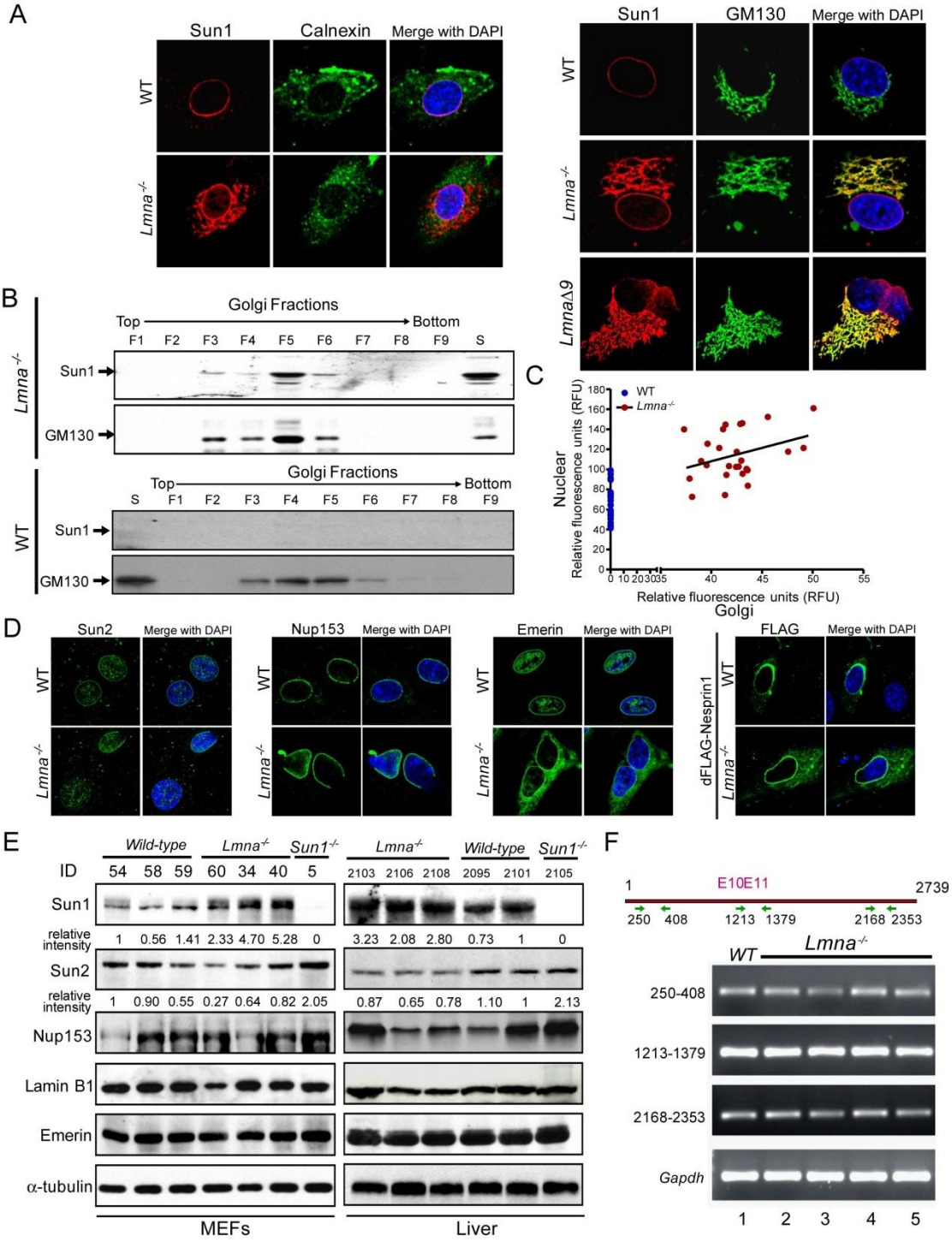

Supplemental Figure S2. Loss of lamin A correlates with Sun1 accumulation in the NE and Golgi (related to Figure 3).

(A) *Lmna*$^{-/-}$ MEFs or *Lmna*Δ9 MAFs (mouse adult fibroblasts) were stained with anti-Sun1 (red) and anti-GM130 (a Golgi marker; green; right middle panels) or anti-Calnexin (an ER marker; green; left middle panels). DAPI staining of DNA is in blue. Yellow in merged panels indicates Sun1 colocalization with GM130 in the Golgi, and

absence of colocalization with Calnexin in the ER. Localization of Sun1 in the Golgi was observed in *Lmna*$^{-/-}$ and *Lmna*Δ9 cells. Images are summations of z-stacks.

(B) Golgi preparation using cytosolic lysate (S) from *Lmna*$^{-/-}$ liver tissue was fractionated on a sucrose density gradient; the Golgi fractions (F1-F9) were examined together and compared to total loading cytosolic lysate (S) by immunoblotting using anti-mouse Sun1 and anti-Golgi marker GM130, respectively. The mouse Sun1 protein co-fractionated with Golgi constituent protein GM130. Golgi preparation from WT liver tissue fractionated in the same way is shown as control at the bottom. Unlike *Lmna*$^{-/-}$ liver cytosol, minimal Sun1 signal was detected in the WT cytosolic lysate (S).

(C) Correlation of Sun1 staining in the nucleus and Golgi in WT and *Lmna*$^{-/-}$ MEFs. Linear regression indicates a positive correlation (slope=0.375) between Sun1 in the nucleus and in the Golgi in *Lmna*$^{-/-}$ MEFs.

(D) Confocal immunofluroscent localization of cell endogenous Sun2, Nup153, Emerin and transfected human Nesprin1 (accession no. NM_133650, 982 a.a.) in WT and *Lmna*$^{-/-}$ MEFs. Nuclear envelope localization of Sun2 and Nup153 was not perturbed by *Lmna* depletion while some increased cytoplasmic distribution of Emerin and Nesprin1 was seen in *Lmna*$^{-/-}$ MEFs. No workable antibody that recognizes cell endogenous Nespirin1 was available; so the analysis was performed with FLAG-tagged transfected Nespirin1 stained with anti-FLAG.

(E) Western blotting of Sun1, Sun2, Nup153, lamin B1, Emerin and α-tubulin in MEFs (left) and mouse liver tissue (right). Wild type, *Lmna*$^{-/-}$, and *Sun1*$^{-/-}$ samples were compared. Mouse identification (ID) numbers indicate individual animals. Aside from Sun1, no consistent difference was noted between *Lmna*$^{-/-}$ and WT cells or liver tissues.

(F) RT-PCR analysis of *Sun1* mRNA (nucleotides 250-408, 1213-1379 and 2168-2353) from wild type (lane 1) and four individual *Lmna*$^{-/-}$ (lanes 2-5) MEFs. *Gapdh* is shown as control.

Suppl Figure S3.

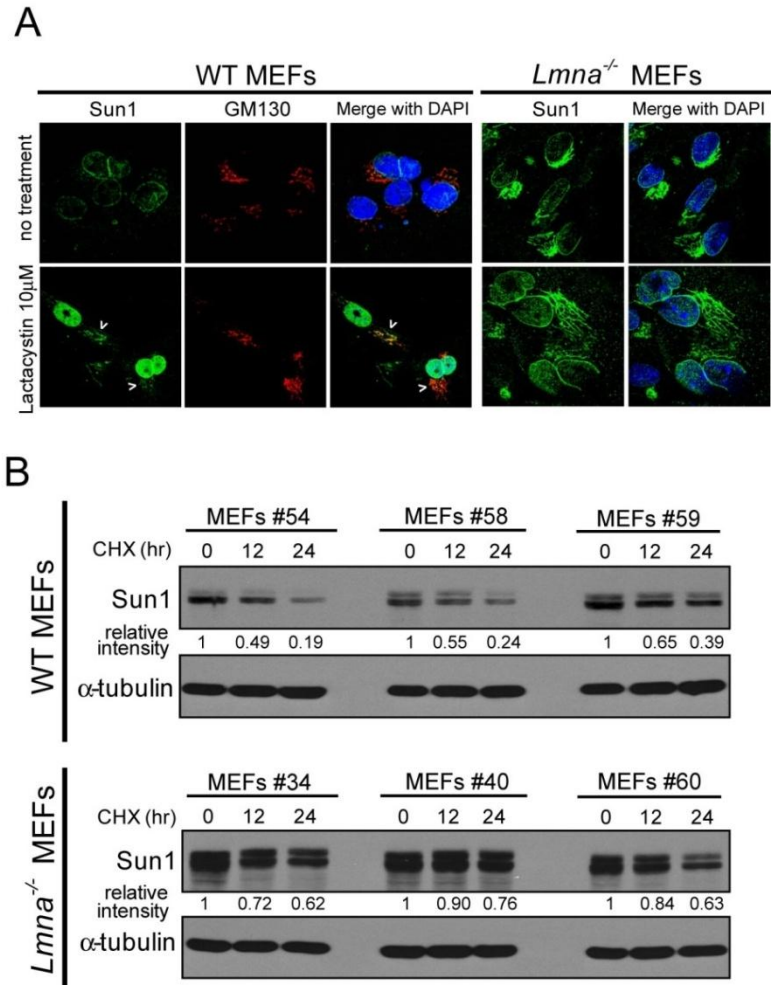

Supplemental Figure S3. Analyses of Sun1 protein turnover (related to Figure 3). (A) Immunofluorescence images of wild type MEFs and *Lmna*$^{-/-}$ MEFs treated without or with 10 μM of lactacystin (for 14 hours). Cells were fixed and co-immunostained with rabbit anti-mSun1 (green) and mouse anti-GM130 (red) antibodies. DNA is in blue. Increased Sun1 is seen in the nucleus with some protein found in extranuclear locale of WT MEFs (in 10-15% of cells, indicated by arrow heads) after lactacystin treatment. In lactacystin treated WT MEFs, Sun1 accumulation was observed in the nuclear membrane with a circumferential pattern and in the nucleoplasm with a punctate pattern. In *Lmna*$^{-/-}$ MEFs, Sun1 accumulation in the nucleus and in the Golgi is increased after lactacystin treatment.

(B) Western blotting of Sun1 in wild type and *Lmna*$^{-/-}$ MEFs treated without or with 25 μg/mL cycloheximide (for 12 or 24 hours); α-tubulin was used as a normalization control. Relative amounts of Sun1 were calculated and shown in the numbers below the blot. The half life of the Sun1 protein is approximately 12 hours in WT MEFs and

is calculated to approximate >24 hours in *Lmna*$^{-/-}$ MEFs.

Suppl Figure S4.

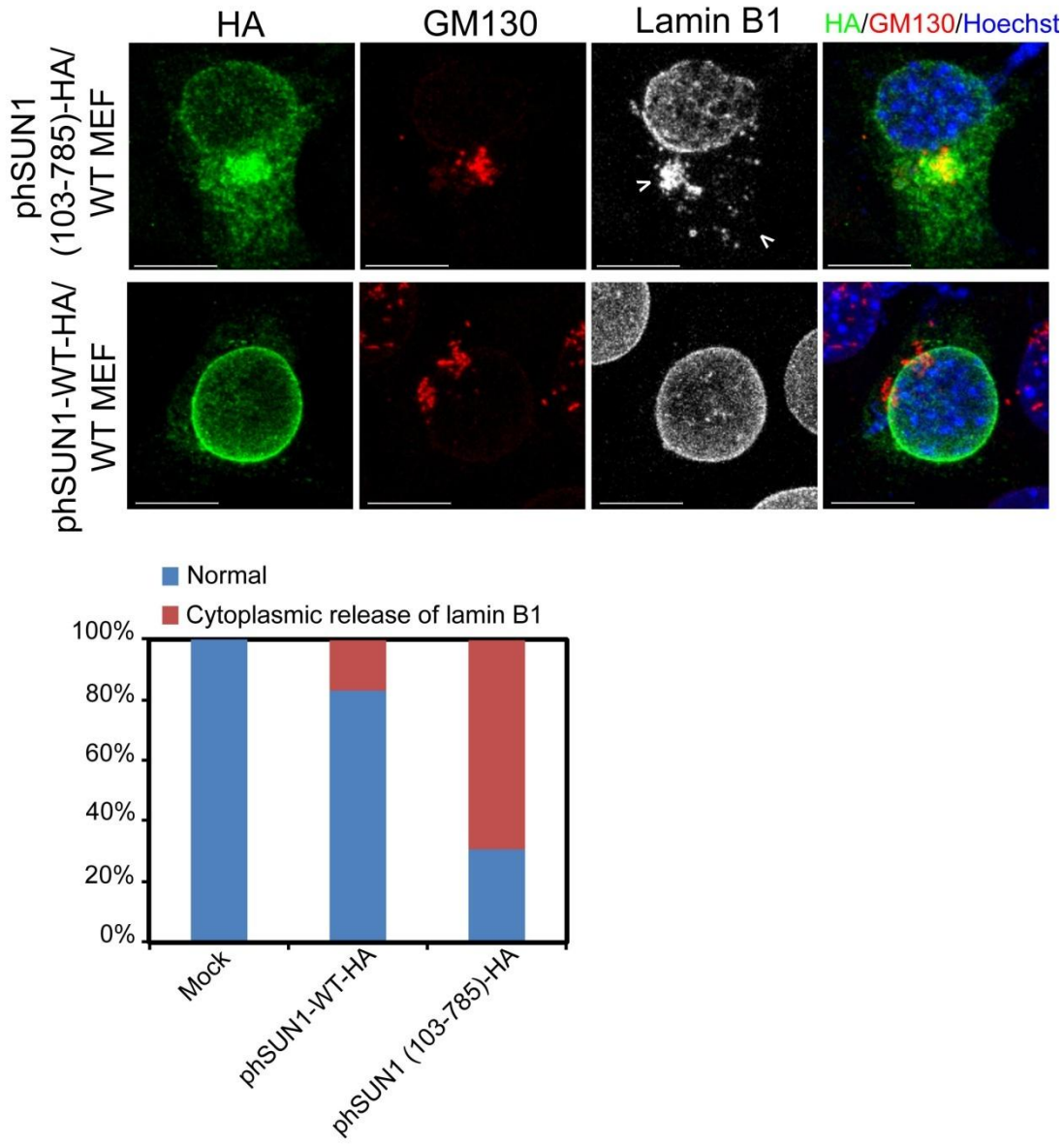

Supplemental Figure S4. Human SUN1 deleted for its N-terminal lamin A-interacting domain locates in the Golgi (related to Figure 4).

(Top) Localization of WT or N-terminal deletion (amino acids 103-785) mutant of HA-tagged human SUN1 in MEFs. Cells were co-immunostained with mouse anti-HA (green), rabbit anti-GM130 (red) and goat anti-lamin B1 (grey scale). DNA was stained with Hoechst33342 (blue). SUN1 (103-785) mutant protein localizes to extranuclear Golgi; while WT SUN1 is in the nuclear membrane. The arrowheads denote cytoplasmic lamin B1. Bars, 10 μm. (Bottom) Quantification of MEF cells with cytoplasmic release of lamin B1 in MEFs after 30 hours of transfection of HA-tagged wild type human SUN1 or the SUN1 (103-785) mutant protein. One hundred cells were counted in each case.

Suppl Figure S5.

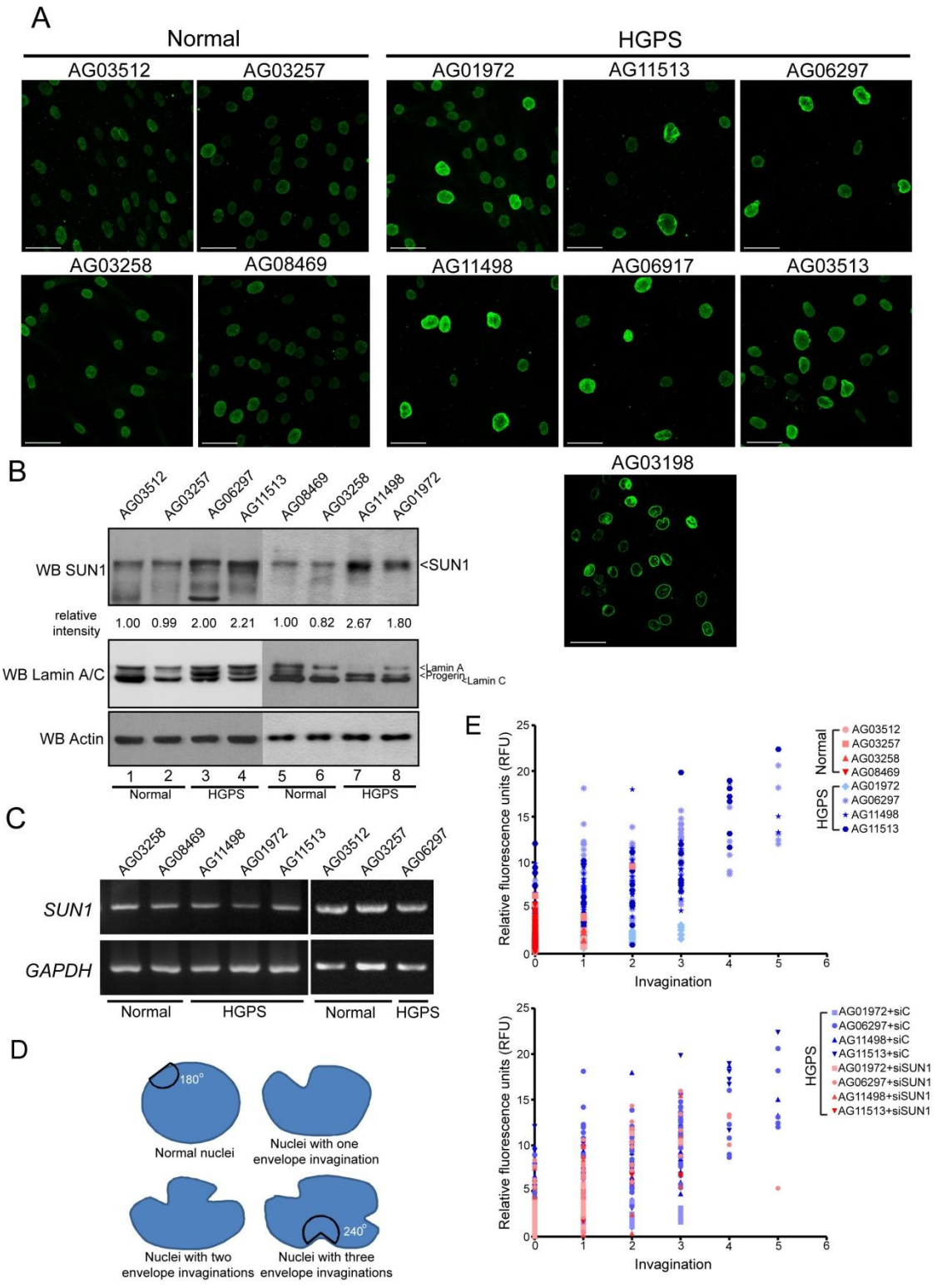

Supplemental Figure S5. Properties of normal human and Hutchinson-Gilford progeria syndrome (HGPS) skin fibroblasts (related to Figure 6).

(A) Immunofluorescent SUN1 staining images of multiple cells from four normal (AG03512, AG03257, AG03258, AG08469) and seven HGPS (AG01972, AG11513, AG06297, AG11498, AG06917, AG11513, AG03198) fibroblasts (Table S1). Note that the increased expression of SUN1 is seen in all HGPS samples with one-third or more of cells in each HGPS visual field staining brightly green. Bars, 50 μm.

(B) Expression of SUN1, lamin A/C and progerin in normal and representative HGPS skin fibroblasts was assessed by Western blotting. Progerin which is deleted for 50 amino acids from full length lamin A runs slightly faster in SDS-PAGE. Relative intensities of SUN1 expression levels compared to AG03512 (lanes 2-4) or AG08469 (lanes 6-8) are indicated in the numbers below the top panel.

(C) Expression of *SUN1* mRNA in normal and representative HGPS skin fibroblasts by RT-PCR. *GAPDH* was used for normalization.

(D) A cartoon of nuclei with shapes and contour changes that are scored as nuclear invaginations. Nuclei with $>240^{o}$ contour changes are scored as aberrant invagination(s).

(E) Distribution of nuclear invaginations in normal and HGPS skin fibroblasts (as presented in Figure 5B-D) treated with control (siC) or SUN1 siRNA (siSUN1). Significantly higher numbers of aberrant nuclear invaginations ($P < 0.001$) were seen for each of the HGPS cells compared to control AG03512 (normal skin fibroblasts, t-test); similarly, significantly lower numbers of nuclear invaginations ($P < 0.0001$) were seen for all HGPS cells treated with SUN1-RNAi compare to Control-RNAi treated cells (t-test). RFU are relative fluorescent units of staining for SUN1.

Suppl Figure S6.

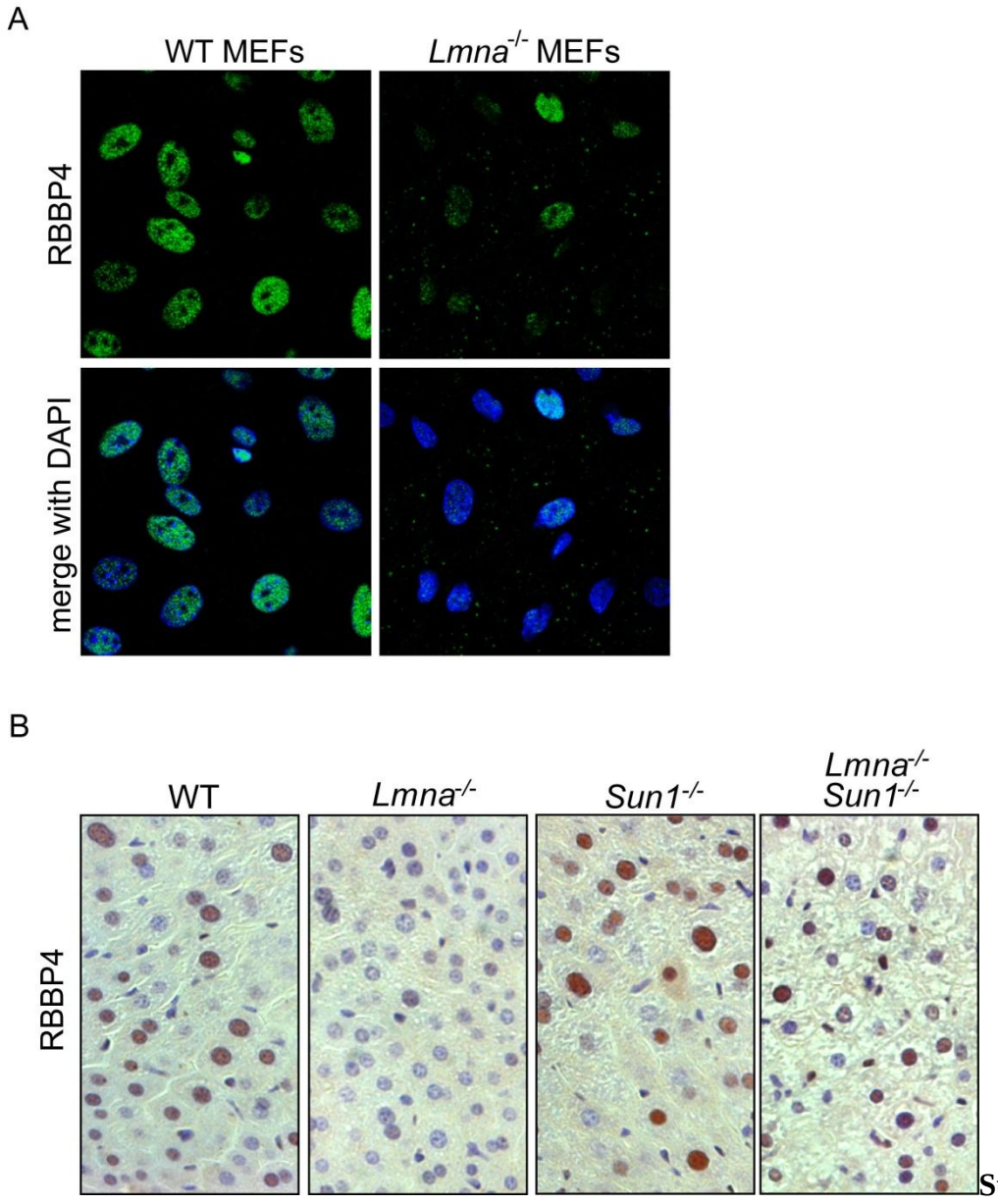

Supplemental Figure S6. *Lmna*$^{-/-}$*Sun1*$^{-/-}$ and WT mouse liver tissue show more RBBP4 staining than *Lmna*$^{-/-}$ liver tissue (related to Figure 7).

(A) WT and *Lmna*$^{-/-}$ MEFs were stained with rabbit anti-RBBP4 (green). Note the reduced staining for RBBP4 in *Lmna*$^{-/-}$ MEFs. DAPI staining of DNA is in blue.

(B) Liver tissue from WT, *Lmna*$^{-/-}$, *Sun1*$^{-/-}$ and *Lmna*$^{-/-}$*Sun1*$^{-/-}$ was stained with RBBP4 by immunohistochemistry. Brown signals show nuclear RBBP4 staining; note fewer numbers of "brown" nuclei in *Lmna*$^{-/-}$ liver compared to WT, *Sun1*$^{-/-}$ and *Lmna*$^{-/-}$ *Sun1*$^{-/-}$ liver. Images are at 400× magnification.

SUPPLEMENTAL EXPERIMENTAL PROCEDURES

Cell culture

Normal (AG03512, AG03257, AG03258, AG08469) and HGPS (AG01972, AG06297, AG11498, AG11513, AG06917, AG03513, AG03198) human skin fibroblasts were from the National Institute of Aging (NIA) Aged Cell Repository distributed by the Coriell Institute. Cells were maintained in high glucose MEM containing 10-15% FBS and supplemented with 2 mM L-glutamine, 1 mM sodium pyruvate and antibiotics. Mouse embryonic fibroblasts (MEFs) were prepared from E15.5 embryos. Cells were dissociated by trypsin and were maintained in Dulbecco's modified eagle medium (DMEM) supplemented with 15% fetal bovine serum (FBS), 2 mM L-glutamine and antibiotics.

Plasmids

The mouse Sun1 (mSun1, accession number: NM_024451, 913 a. a.), mSun1-FLAG, mSun1-Tgn38-HA, full length human SUN1 (hSUN1-HA, accession number: NM_001130965, 785 a. a.), hSUN1 (a.a. 103-785)-HA and mouse lamin A expression plasmids were constructed based on the pcDNA3.1 vector (Invitrogen). All the constructs generated were verified by DNA sequencing, and the expression of the cloned genes was confirmed by Western analyses. Lipofectamine^{TM} 2000 (Invitrogen) and PolyJet^{TM} (SignaGen Laboratories) were used for plasmid transfections.

Reagents, Primers, and RT-PCR

Regents were obtained from the following resources. Sigma-Aldrich: nocodazole (M1404), lactacystin (L6785), brefeldin A (BFA, B5936), latrunculin B (LAT-B, L5288), cycloheximide (C4859). Primer sequences for *Sun1* genotyping: 5'-GGCAAGTGGATCTCTTGTGAATTCTTGAC-3' and 5'-GTAGCACCCACCTTGGTGAGCTGGTAC-3'. Wild type mice produced a 1262 bp fragment and the *Sun1* knockout mice produced a 263 bp fragment. Primer sequences for *Lmna* genotyping: common forward primer for WT and *Lmna* KO 5'-AGTTCGTGCGGCTGCGCAACAAGTCCAACG-3'; reverse primer for WT: 5'-GTCATCAAAGGATCGTCACCATTCTGAC-3'; reverse primer for *Lmna* KO: 5'-CCATTCGACCACCAAGCGAAACATCGC-3'. Wild type mice produced a 500 bp fragment and the *Lmna* knockout mice produced a 850 bp fragment.

For RT-PCR, total RNA was extracted from MEFs using TRIzol (Invitrogen). Complementary DNA (cDNA) was produced from MEFs RNA (5 μg) using the SuperScript II Reverse Transcriptase Kit (Invitrogen). Three pairs of primer p177/p178 (p177: 5'-GGGACAGCCAGGCTATTGATT; p178: 5'-CATGGCTTGTGCTCGAGGA)**,** p1213/p1379 (p1213: 5'-CTTCTTACCAGGTGCCTTCG; p1379:5'GAATCGTCCACCCTCTGTGT), and

p140/p141 (p140: 5'-TATTGTGTCTGCCGTGAATC; p141: 5'-GCCGTCTTGGTCTCATAGGTC) (Ostlund et al., 2009) were used to amplify three coding regions of mouse Sun1, respectively. PCR products of mouse glyceraldehyde-3-phosphate dehydrogenase (Gapdh-F: 5'- TCACCACCATGGAGAAGGC; Gapdh-R: 5'- GCTAAGCAGTTGGTGGTGCA) were served as an internal control. Primers for RT-PCR of human *SUN1* (hsSUN1-F: 5'-GGACGTGTTTAAACCCACGACTTCTCG; hsSUN1-R: 5'-CTCTGACTTTAGCTGATCCAGCTCCAGC), human *GAPDH* (GAPDH-F: 5'-AGCCACATCGCTCAGACACC; GAPDH-R: 5'-GTACTCAGCGGCCAGCATCG).

Antibodies

The rabbit anti-SUN domain of mouse Sun1 (a.a. 701-913) was prepared as described in Chi *et al*. (Chi et al., 2009). Specificity of this antibody in Western blot and immunofluorescence staining was examined and verified by comparing the signals from wild type and *Sun1*$^{-/-}$ MEFs. The rabbit anti-human SUN1 antibody was prepared as described previously (Chi et al., 2007). Other antibodies were obtained from the following resources. Abcam: rabbit anti-GM130 (ab52649), rabbit anti-H3K9me3 (ab8898), rabbit anti-Sun2 (ab87036), mouse anti-RBBP4 (ab488); Sigma-Aldrich: mouse anti-αtubulin (T5168), mouse anti-Actin (A1978), mouse anti-HA

(H3663), mouse anti-FLAG (F1804), rabbit anti-FLAG (F7425), rabbit anti-GM130 (G7295); Santa Cruz Biotechnology: mouse anti-lamin A/C (sc-7292), goat anti-lamin B1 (sc-6217), rabbit anti-Emerin (sc-15378); Covance: mouse anti-Nup153 (MMS-102P), mouse anti-human SUN1 (customized); Epitomics: rabbit anti-RBBP4 (2599-1). BD Transduction Laboratories: mouse anti-Calnexin (610524); mouse anti-GM130 (610823).

Western blotting

To extract nuclear envelope proteins from human skin fibroblasts, cultured cells were washed twice with PBS. The cell pellet was incubated with ice-cold RIPA buffer [50 mM HEPES, pH 7.3, 150 mM NaCl, 2 mM EDTA, 20 mM β-gylcerophosphate, 0.1 mM Na_3VO_4, 1mM NaF, 0.5 mM DTT and protease inhibitor cocktail (Roche)] containing 1% NP-40 and 1% SDS plus mild sonication. Lysates were then analyzed by 8% SDS-PAGE, transferred to polyvinylidene fluoride (PVDF, Millipore) membrane and blotted antibodies. Corresponding alkaline phosphatase-conjugated secondary antibodies (Sigma-Aldrich) were added, and the blots were developed by chemiluminescence following the manufacturer's protocol (Chemicon).

RNAi

Synthetic Stealth siRNA duplexes targeting human *SUN1* (5'-CCAUCCUGAGUAUACCUGUCUGUAU-3') (Chi et al., 2007) were from Invitrogen. Small interfering RNAs were induced into human skin fibroblasts using the Lipofectamine 2000 transfection reagent (Invitrogen) or Lipofectamine RNAiMax trasnfection reagent (Invitrogen). For siRNA delivery using Lipofectamine 2000, 60 pmol of siRNA mixed with 3 μL of Lipofectamine 2000 transfection reagent were used per well in a 12-well plate. For Lipofectamine RNAimax for siRNA delivery, only 3 pmol and 2 μL of the transfection reagent were used per well in a 12-well plate.

Golgi fractionation

Golgi fractionation was performed using the Golgi isolation kit (Sigma-Aldrich, GL0010) according to the manufacturer's protocol with some modifications. Mouse liver was minced with 1 mL of 0.25 M sucrose isolation solution per 1 g of tissue. The tissue suspension was homogenized with 6 slow motions of the PTFE pestle at 300 rpm and centrifuged at 3,000×g for 15 minutes at 4 °C. Supernatant was transferred to a fresh tube and concentration of sucrose was adjusted to 1.25 M. A discontinuous gradient was built in an ultracentrifuge tube by adding 1.84 M sucrose solution, the sample (sucrose concentration adjusted to 1.25 M), 1.1 M sucrose

solution and 0.25 M sucrose solution sequentially. After centrifugation at 12,000×g for 3 hours, the Golgi-enriched fraction from the 1.1 M/0.25 M sucrose interphase was withdrawn and subjected to Western analyses.

Senescence assay

The senescence associated β-galactosidase (SA-β-Gal) assay was performed by following protocol of the Cellular Senescence Assay Kit from Cell Biolabs, Inc.

Cell proliferation assay

Cell proliferation was performed by quantifying viable cells with Cell Counting Kit-8 (Fluka) according to the manufacturer's protocol.

Micro-CT (computer tomography)

Wild type, *Sun1*$^{-/-}$, *Lmna*$^{-/-}$ and *Lmna*$^{-/-}$*Sun1*$^{-/-}$ mice were examined by compact cone-beam tomography (MicroCAT-II scanner). Whole-body scans were performed in the axial plane with the specimens mounted in a cylindrical sample holder. MicroCT was performed at 55 kVp, with an anode current of 500 μA and a shutter speed of 500 msec. The femur bone specimens were fixed in 10% formalin buffered with phosphate and then examined by SkyScan 1172 Micro-CT. Three-dimensional images of the

skeletons were reconstructed from the micro-CT scanning slices and used for analyses of the skeletal structure and morphology. Quantitative data were calculated by SkyScan CT-analyser Software Guide. A manufacturer-provided hydroxyapatite phantom of known density was used to calibrate the mean density of bone volume and the cortical thickness.

MRI (magnetic resonance imaging)

Mouse cardiac magnetic resonance imaging (MRI) was conducted by following the NIH animal care and use guidelines. MRI experiments were performed in a 7.0T, 16-cm horizontal Bruker MR imaging system (Bruker) equipped with Bruker ParaVision 4.0 software. Mice were anesthesized with 1.5-3 % isoflurane and imaged with ECG, temperature and respiratory detection using a 38 mm Bruker birdcage volume coil. Magnevist (gadopentate dimeglumine contrast agent, Bayer HealthCare) diluted 1:10 with sterile 0.9% saline, was administered subcutaneously at 0.3 mmol Gd/kg. Intravenous route was not used due to small size of some mice (ca. 10-12g) with invisible tail veins. T1 weighted gradient echo cine images of the heart were acquired in short axis from above the base to the apex (6-10 slices depending on slice thickness) with the following parameters: repetition time TR = 11 ms, echo time TE= 3.5 ms, 11 to 14 frames, 30 degree flip angle, 2.8 to 3.0 cm field of view, 256×256

matrix, respiratory and ECG-gated. 1.0 mm slice thickness with 4-5 averages was used on mice over 12 g and 0.75 mm thickness with 4-7 averages for mice less than 12 g. Cardiac MRI data were processed to determine ejection fractions and associated functional parameters using the CAAS-MRV-FARM software (Pie Medical Imaging, Netherlands.)

Statistics

Means and standard deviation are presented to describe the distribution. Student t test was used to compare mean difference between two groups. ANOVA analysis was performed to compare mean difference among groups. Multiple comparisons were carried out by Scheffe's Test. Kaplan-Meier method was used to draw the survival curves. Log-rank test was conducted on the homogeneity of survival curves among four types of mouse. We used Mixed model to compare the difference between body weight during the followed period among four types of mouse. We also used Generalized Estimating Equations (GEE) Method to compare the cell number among four types of MEF cells. The working correlation structure was set unstructured, and the linked function was set Poission distribution. Statistics were carried out by SAS 9.2 or GraphPad Prism 5.0.

Supplemental Figure 1

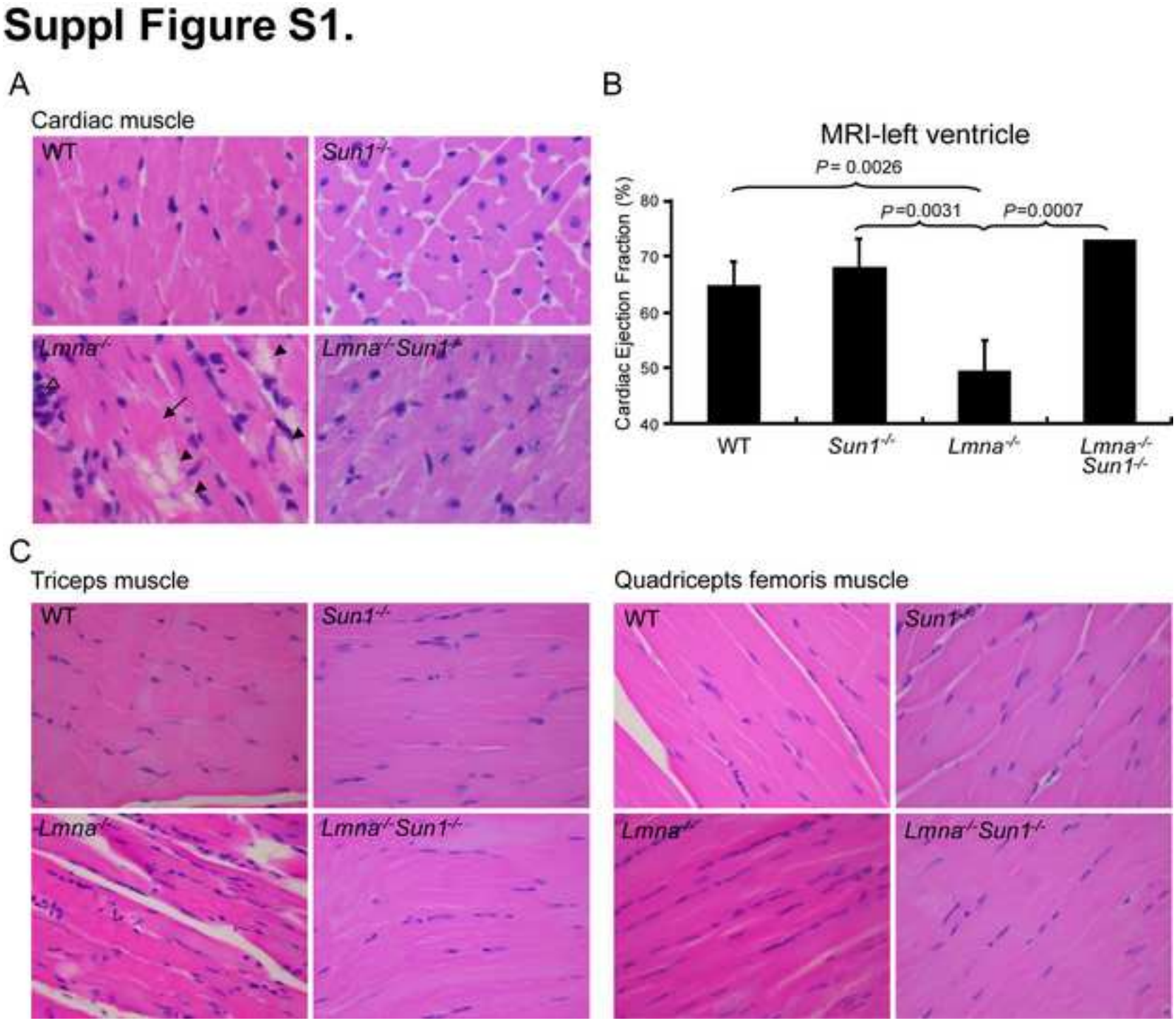

Supplemental Figure 2

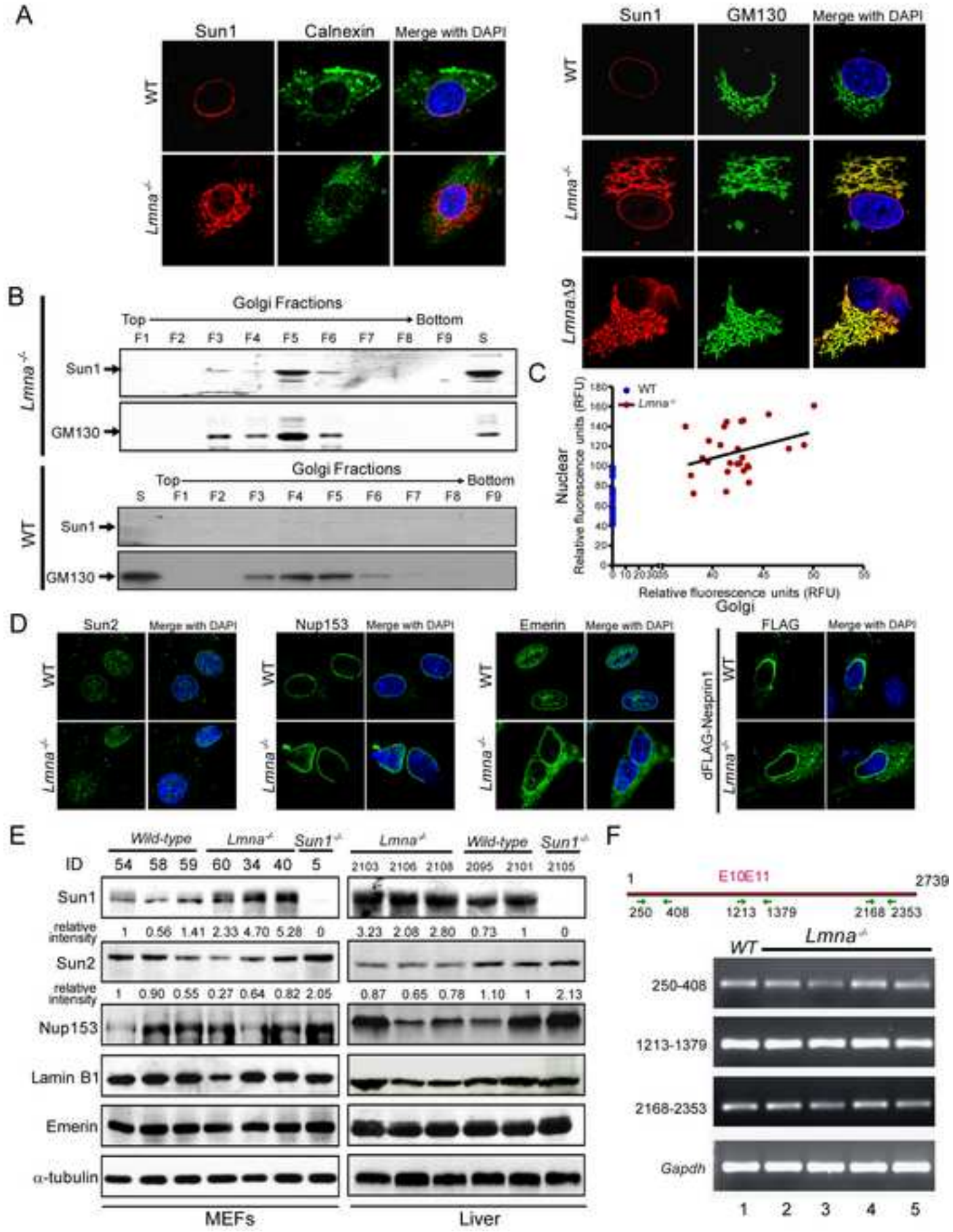

Supplemental Figure 3

Suppl Figure S3.

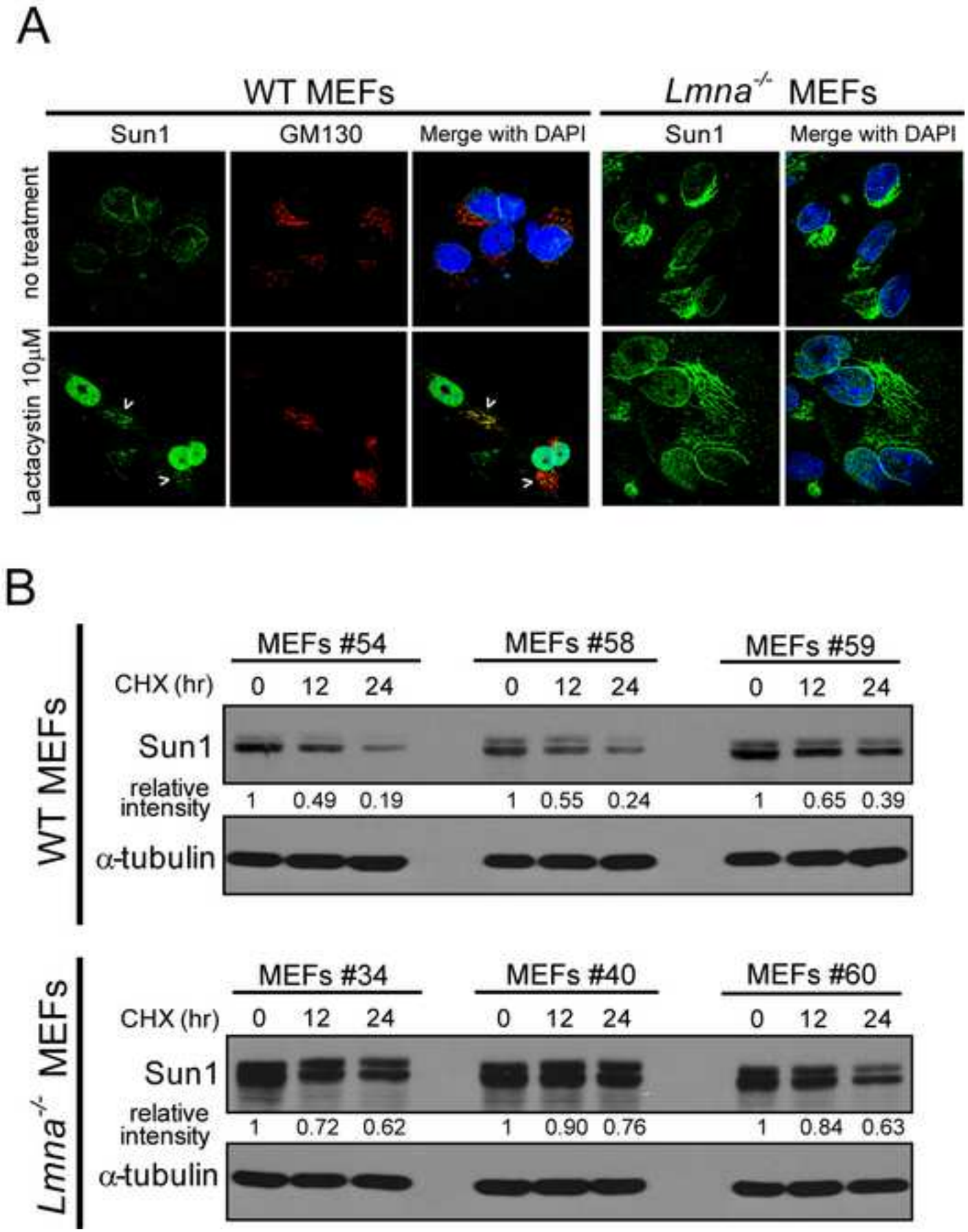

Supplemental Figure 4

Suppl Figure S4.

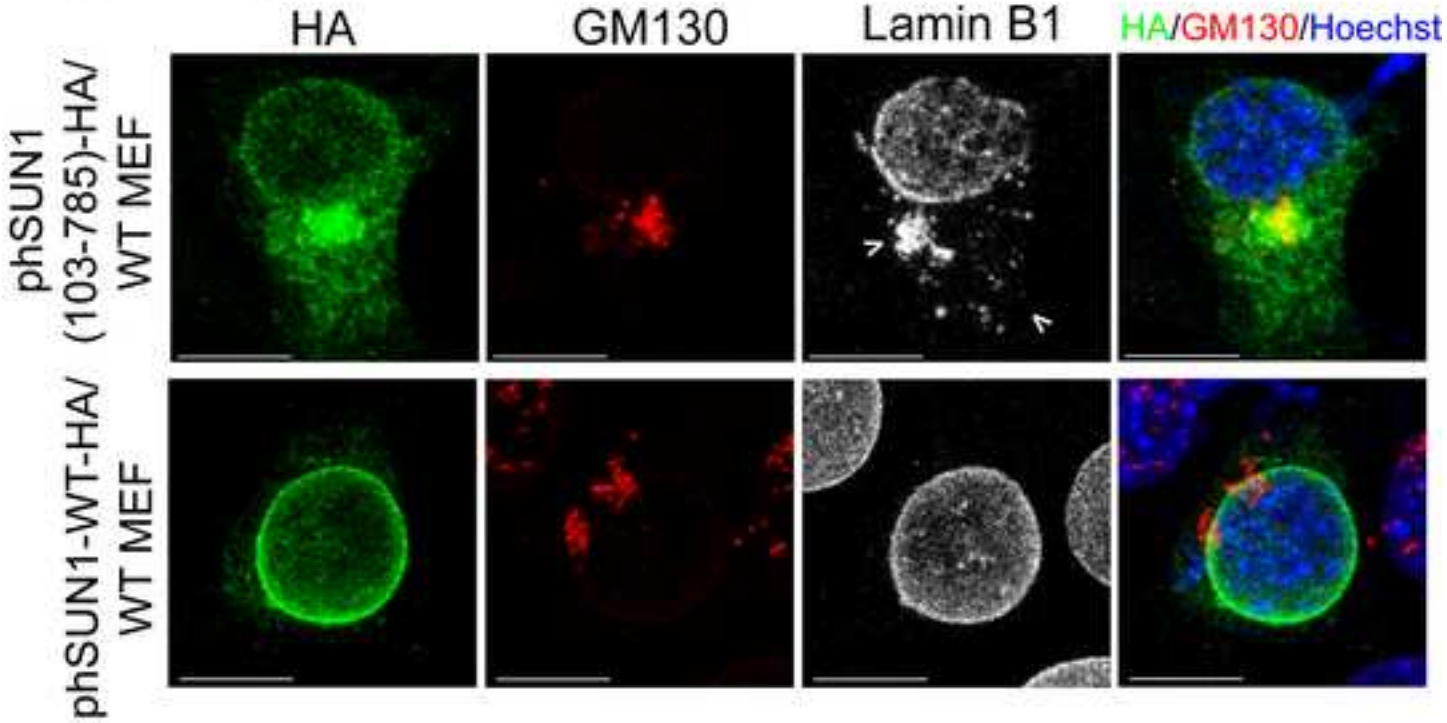

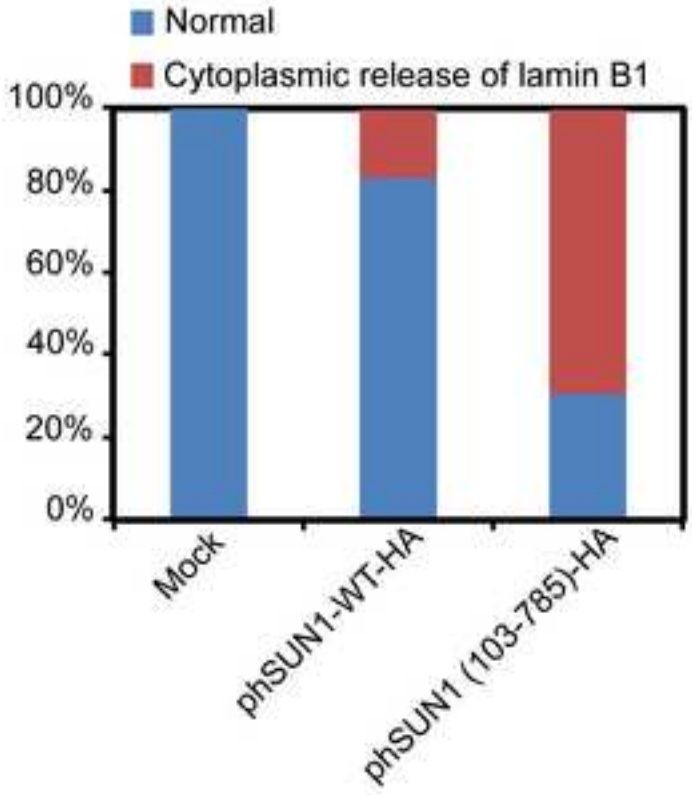

Supplemental Figure 5

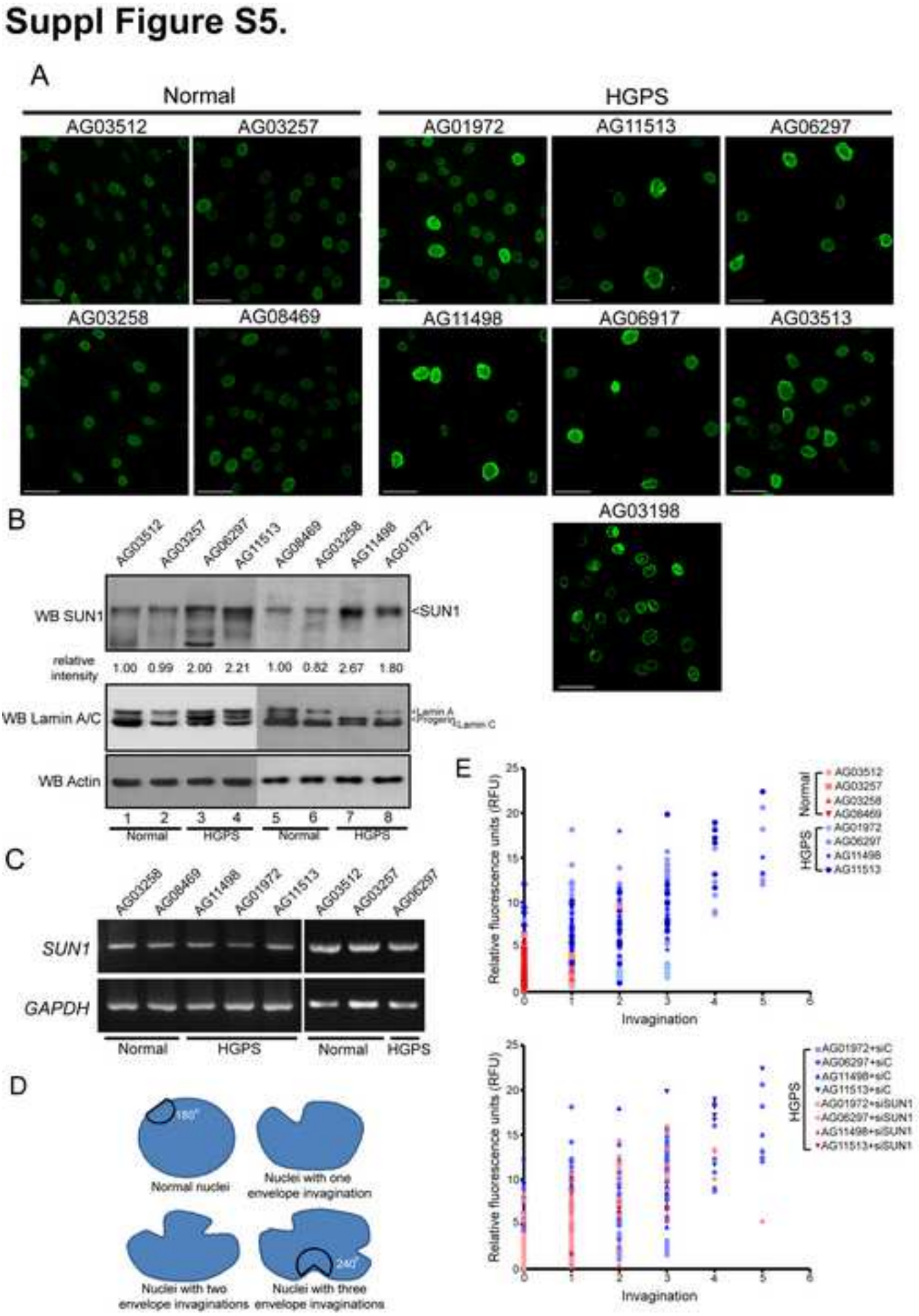

Supplemental Figure 6

Suppl Figure S6.